# Decoupling multimode vibrational relaxations in multi-component gas mixtures: Analysis of sound relaxational absorption spectra*

Zhang Ke-Sheng(张克声), Wang Shu(王 殊), Zhu Ming(朱 明)†, Ding Yi(丁 毅), and Hu Yi(胡 轶)

*Department of Electronics and Information Engineering, Huazhong University of Science and Technology, Wuhan* 430074, *China*

(Received 27 July 2012; revised manuscript received 6 September 2012)

Decoupling the complicated vibrational–vibrational (V–V) coupling of a multimode vibrational relaxation remains a challenge for analyzing the sound relaxational absorption in multi-component gas mixtures. In our previous work [*Acta Phys. Sin.* **61** 174301 (2012)], an analytical model to predict the sound absorption from vibrational relaxation in a gas medium is proposed. In this paper, we develop the model to decouple the V–V coupled energy to each vibrational–translational deexcitation path, and analyze how the multimode relaxations form the peaks of sound absorption spectra in gas mixtures. We prove that a multimode relaxation is the sum of its decoupled single-relaxation processes, and only the decoupled process with a significant isochoric-molar-heat can be observed as an absorption peak. The decoupling model clarifies the essential processes behind the peaks in spectra arising from the multimode relaxations in multi-component gas mixtures. The simulation validates the proposed decoupling model.

**Keywords:** vibrational relaxation, sound absorption, vibrational–vibrational coupling, decoupled single-relaxation process

**PACS:** 43.35.Ae, 43.35.Fj **DOI:** 10.1088/1674-1056/22/1/014305

## 1. Introduction

The molecular vibrational relaxation model for excitable gases (non-monatomic gases or gas mixtures) has been developed to analyze sound relaxational absorption over the past 90 years.[1–3] In most cases, an excitable gas medium has two or more types of molecular vibrational modes. Those modes will arouse a multimode vibrational relaxation which is synthesized by a strong vibrational–vibrational (V–V) energy coupling with the passage of sound waves.[1–5] The sound absorption spectra due to multimode relaxations generally display only one peak, or occasionally two peaks.[1–3,6–9] Finding the correspondence between the complicated V–V coupling and the concise presentation of a few peaks of the spectrum in a multi-component gas mixture still remains an important challenge for understanding the sound relaxational absorption behavior. Decoupling the V–V coupling for multimode relaxation provides a way to address this problem.

Over the years, some decoupling theories have been proposed. Bauer provided a phenomenological theory to decouple the coupled V–V energy exchanges by using a main axis transformation of the effective adiabatic compressibility in pure polyatomic gases.[2] Shields suggested another phenomenological theory on the basis of the experimental relaxation time to decouple the multimode relaxation in binary-gas mixtures.[7] Bass acquired a model of decoupled effective specific heats based on the eigenproperties of the coupled energy relaxation matrices in pure polyatomic gases or binary diatomic mixtures.[4] However, all the decoupling theories above cannot be used to analyze the multi-component mixture. Later, Dain *et al.* (DL)[8,9] employed the coupled relaxation equations given by Schwartz *et al.* (SSH)[10] to ternary gas mixtures. Unfortunately, the DL model only provides a numerical calculation for the sound absorption spectra as a result of the V–V coupling, which cannot be applied to decouple a multimode relaxation.

Recently, we presented an analytical model based on the V–V coupling to calculate the sound absorption spectrum.[3] In this paper, a analytical model will be developed to decouple multimode relaxations in multi-component gas mixtures. The motivation is to decouple the V–V coupled energy among all the vibrational modes into the vibrational–translational (V–T) deexcitation paths or the decoupled single-relaxation processes. Based on this decoupling model, we give a quantitative analysis, showing how a multimode relaxation leads to peaks of the sound absorption spectrum in a multi-component gas mixture around room temperature. This work discloses that a multimode relaxation is the sum of its decoupled processes, and the characteristics of the decoupled processes determine the features of the sound absorption spectrum.

In Section 2, we obtain a coupled expression of effective isochoric-molar-heat in a multi-component mixture. In Section 3, we decouple a multimode vibrational relaxation to a

*Project supported by the National Natural Science Foundation of China (Grant Nos. 60971009 and 61001011), the Specialized Research Fund for the Doctoral Program of Higher Education of China (Grant No. 20090142110019), the Natural Science Foundation of Hubei Province, China (Grant No. 2010CDB02701), and the Fundamental Research Funds for the Central Universities, China (Grant No. 2012QN083).

†Corresponding author. E-mail: zhuming@mail.hust.edu.cn

© 2013 Chinese Physical Society and IOP Publishing Ltd 

group of single-relaxation processes. In Section 4, we compare the predicted sound absorption spectra with the experimental data, and analyze how the characteristics of the decoupled processes influence the features of the peaks in the spectra. Conclusions are given in Section 5.

## 2. Coupled expression of multimode vibrational relaxation

### 2.1. Effective isochoric molar heat due to one-mode vibrational relaxation

The lag in distribution of energy between internal and external degrees of freedom (DOF) essentially contributes to the molecular thermal relaxation.[1,11] The macroscopic footprint of this lag is explicitly displayed in the frequency dependence of effective isochoric molar heat (IMH) of excitable gases.[6,12]

According to the theory of Herzfeld and Litovitz,[11] the total thermodynamic energy change of gas resulting from the sound propagation can be divided into two parts: one belongs to the external DOF; the other belongs to the internal DOF. In the study of vibrational relaxation, the rapid equilibration between rotation and translation makes the (V–R)+(R–T) process equal to the V–T process.[7] Hence, the rotation is conventionally classified as the translation as the external DOF to differentiate from the vibration, which is classified as the internal DOF and takes a longer time for adjustment.[11] Then, if there is only one vibrational mode in a gas, the change of its thermodynamic energy is[11]

$$\begin{aligned} \mathrm{d}E &= C_V^{\mathrm{eff}}\,\mathrm{d}T \\ &= C_V^{\infty}\,\mathrm{d}T + C_V^{\mathrm{vib}}\,\mathrm{d}T^{\mathrm{vib}} \\ &= \left(C_V^{\infty} + C_V^{\mathrm{vib}}\frac{\mathrm{d}T^{\mathrm{vib}}}{\mathrm{d}T}\right)\mathrm{d}T, \end{aligned} \tag{1}$$

where $E$ is the thermodynamic energy of the gas; $T$ and $T^{\mathrm{vib}}$ are the instantaneous temperatures of the external (translation and rotation) and the internal (vibration) DOFs, respectively; $C_V^{\mathrm{eff}}$ is the effective IMH; $C_V^{\infty}$ is the non-relaxing part of the IMH; and $C_V^{\mathrm{vib}}$ is the vibrational IMH.

The $C_V^{\infty}$ is only dependent on the molecular symmetry.[6] For a linear molecule, there are 3 translations and 2 rotations, so $C_V^{\infty} = 5R/2$ ($R$ is the universal gas constant); for a nonlinear molecule, $C_V^{\infty} = 3R$. The $C_V^{\mathrm{vib}}$ is given by the Planck–Einstein function for a harmonic oscillator[8]

$$C_V^{\mathrm{vib}} = gR\left(\frac{\theta^{\mathrm{vib}}}{T_0}\right)\frac{\exp(\theta^{\mathrm{vib}}/T_0)}{(\exp(\theta^{\mathrm{vib}}/T_0)-1)^2},\quad \theta^{\mathrm{vib}} = \frac{h\upsilon}{k_{\mathrm{B}}}, \tag{2}$$

where $h$ is Planck's constant; $k_{\mathrm{B}}$ is Boltzmann's constant; $T_0$ is the equilibrium temperature; $\theta^{\mathrm{vib}}$, $\upsilon$, and $g$ are the characteristic temperature, the characteristic frequency, and the degeneracy of the vibrational mode, respectively.

### 2.2. Coupled expression of effective IMH due to multimode vibrational relaxation[3]

In a gas mixture, the total change of thermodynamic energy caused by the sound propagation is the sum of the energy changes of all kinds of molecular DOFs. The acoustic energy stored in the external DOFs of different molecules is in phase with the sound wave, and hence the temperature fluctuations of all external DOFs are treated as the same.[1,8] However, based on Eq. (2), the temperature fluctuations of the internal DOFs are different because different vibrational modes generally possess different characteristic frequencies. Consequently, for a gas mixture with $W$ kinds of molecules, which totally consists of $N$ types of vibrational modes, we can extend Eq. (1) to

$$\begin{aligned} \mathrm{d}E &= C_V^{\mathrm{eff}}\,\mathrm{d}T \\ &= C_{\mathrm{mix}}^{\infty}\,\mathrm{d}T + \sum_{j=1}^{N} a_j C_j^{\mathrm{vib}}\,\mathrm{d}T_j^{\mathrm{vib}} \\ &= \left(C_{\mathrm{mix}}^{\infty} + \sum_{j=1}^{N} a_j C_j^{\mathrm{vib}}\,\mathrm{d}T_j^{\mathrm{vib}}/\mathrm{d}T\right)\mathrm{d}T, \end{aligned} \tag{3}$$

where $C_{\mathrm{mix}}^{\infty} = \sum_{l=1}^{W} a_l C_l^{\infty}$ is the external IMH of the mixture, $C_l^{\infty}$ is the external IMH of molecule $l$, $a_l$ is the mole fraction of molecule $l$ , $\sum_{l=1}^{W} a_l = 1$, $T_j^{\mathrm{vib}}$ is the instantaneous temperature of vibrational mode $j$, $C_j^{\mathrm{vib}}$ is the vibrational IMH of mode $j$, $a_j$ is the mole fraction of mode $j$, and if molecule $l$ contains $N_l$ vibrational modes, these $N_l$ modes share the same mole fraction as $a_l$.

From Eq. (3), we obtain the effective IMH of the mixture

$$C_V^{\mathrm{eff}} = C_{\mathrm{mix}}^{\infty} + \sum_{j=1}^{N} a_j C_j^{\mathrm{vib}} y_j,\quad y_j = \mathrm{d}T_j^{\mathrm{vib}}/\mathrm{d}T, \tag{4}$$

where $y_j$ is the ratio between the temperature fluctuation of vibrational mode $j$ and that of the external DOF. Since there are two or more types of vibrational modes in an excitable gas mixture, the sound passage would give rise to a multimode relaxation. As the result of the V–V coupling, $y_j$ is related with the energy relaxation of all vibrational modes in the mixture. Therefore, equation (4) is the coupled expression of effective IMH.

## 3. Decoupling of multimode vibrational relaxation

### 3.1. Analytical expression for temperature fluctuation ratio between the vibrational mode and external DOF

The temperature fluctuation ratio between the vibrational mode and external DOF, $y_j$, is the result of the V–V coupling. So decoupling $y_j$ is the key to decouple the multimode relaxation in a gas mixture. Moreover, since molecules gain and lose vibrational and translational energies in inelastic collisions, $y_j$ is determined by the molecular vibrational energy relaxation.

The SSH relaxation equations[10] are most widely used to describe the vibrational relaxations in gases quantitatively.[1] The SSH theory concerns the following two kinds of energy transitions: 1) a vibrational–translational energy transfer between the vibrational mode $j$ and the translational DOF of molecule $l$; 2) a vibrational–vibrational energy exchange between vibrational modes $j$ and $k$.

We assume that these two kinds of energy transitions would occur for all vibrational modes in a gas mixture. In terms of the gas mixture with $W$ kinds of molecules and $N$ kinds of vibrations, we extend the SSH–DL coupled relaxation equations[8,10] to a general expression as

$$\begin{aligned}&\frac{\mathrm{d}\Delta T_j^{\mathrm{vib}}}{\mathrm{d}t}\\ &= (\Delta T-\Delta T_j^{\mathrm{vib}})\left[k_{10}(j)+\sum_{\substack{k=1\\k\neq j}}^{N}k_{01}^{10}(j,k)\frac{1-\exp(-h\upsilon_j/k_{\mathrm{B}}T_0)}{1-\exp(-h\upsilon_k/k_{\mathrm{B}}T_0)}\right]\\ &\quad-\sum_{\substack{k=1\\k\neq j}}^{N}(\Delta T-\Delta T_k^{\mathrm{vib}})k_{01}^{10}(j,k)\frac{\upsilon_k}{\upsilon_j}\frac{1-\exp(-h\upsilon_j/k_{\mathrm{B}}T_0)}{1-\exp(-h\upsilon_k/k_{\mathrm{B}}T_0)},\\ &\quad j=1,\ldots,N,\end{aligned}\tag{5}$$

where $\Delta T$ and $\Delta T_j^{\mathrm{vib}}$ denote the fluctuations of the external (or translational) and the vibrational temperatures, respectively; $\upsilon_j$ is the vibrational frequency of mode $j$. The V–T transition rate $k_{10}(j)$ is the number of transitions per second per molecule, and in the transitions, the energy goes from the first-excited-vibrational level to the translational motion, i.e. mode $j$ goes from $1\to 0$ and the vibrational level of molecule $l$ is unaltered,

$$k_{10}(j)=\sum_{l=1}^{W}a_l Z(j,l)\times P_{0-0(l)}^{1-0(j)}\times[1-\exp(-h\upsilon_j/k_{\mathrm{B}}T_0)].\tag{6}$$

The V–V transition rate $k_{01}^{10}(j,k)$ is the rate for the transitions in which mode $j$ goes from $1\to 0$ and mode $k$ from $0\to 1$.

$$k_{01}^{10}(j,k)=a_k Z(j,k)\times P_{0-1(k)}^{1-0(j)}.\tag{7}$$

Here $Z(j,l)$ is the rate of the hard sphere collision[8] between a molecule having mode $j$ and molecule $l$, and $Z(j,k)$ is the rate of the collision between the molecules having modes $j$ and $k$; $P_{0-0(l)}^{1-0(j)}$ and $P_{0-1(k)}^{1-0(j)}$ are respectively the V–T and the V–V transition probabilities, which are calculated by the Tanczos equation.[1,9,13,14]

In Eq. (5), $i\neq j$ means that the V–V energy exchange within a given type of vibrational mode is invalid. From Eq. (5), we can see that every V–V energy exchange couples the differential equations, since the rate at which a given mode relaxes depends on the states of vibrational excitation of all other modes.

In a sound field with a small amplitude, the fluctuations of vibrational and external temperatures are respectively given by[10]

$$\Delta T_j^{\mathrm{vib}}\cong T_j^{\mathrm{vib}}-T_0,\quad \Delta T\cong T-T_0.\tag{8}$$

Since $T-T_0$ varies periodically with time, i.e., is proportional to $\mathrm{e}^{\mathrm{i}\omega t}$, $T_j^{\mathrm{vib}}-T_0$ will also be proportional to $\mathrm{e}^{\mathrm{i}\omega t}$.[11] Then, substituting Eq. (8) into Eq. (5), we obtain the algebraic relaxation equations

$$\begin{aligned}&y_j(k_{jj}+\mathrm{i}\omega)-\sum_{\substack{k=1\\k\neq j}}^{N}y_k k_{jk}=k_{jj}-\sum_{\substack{k=1\\k\neq j}}^{N}k_{jk},\\ &k_{jj}=k_{10}(j)+\sum_{\substack{k=1\\k\neq j}}^{N}k_{01}^{10}(j,k)\frac{1-\exp(-h\upsilon_j/k_{\mathrm{B}}T_0)}{1-\exp(-h\upsilon_k/k_{\mathrm{B}}T_0)},\\ &k_{jk}=k_{01}^{10}(j,k)\frac{\upsilon_k}{\upsilon_j}\frac{1-\exp(-h\upsilon_j/k_{\mathrm{B}}T_0)}{1-\exp(-h\upsilon_k/k_{\mathrm{B}}T_0)},\\ &y_j=\frac{(T_j^{\mathrm{vib}}-T_0)}{(T-T_0)}=\mathrm{d}T_j^{\mathrm{vib}}/\mathrm{d}T,\quad j,k=1,\ldots,N,\ j\neq k.\end{aligned}\tag{9}$$

The algebraic relaxation equations (9) can be expressed in a matrix form as

$$(\boldsymbol{R}+\mathrm{i}\omega\boldsymbol{I})\boldsymbol{y}=\boldsymbol{H},\tag{10}$$

where $y_j=y_j$, $R_{jj}=k_{jj}$, $R_{jk}=-k_{jk}$, $H_j=k_{jj}-\sum_{k=1,k\neq j}^{N}k_{jk}$, $j,k=1,\ldots,N, j\neq k$; and $\boldsymbol{I}$ is the identity matrix. The $\boldsymbol{R}$ is the energy-transition-rate matrix, which can be diagonalized for most cases, that is

$$\boldsymbol{R}=\boldsymbol{V}\boldsymbol{\Lambda}\boldsymbol{V}^{-1},\tag{11}$$

where $\boldsymbol{\Lambda}$ and $\boldsymbol{V}$ are the eigenvalue matrix and the eigenvector matrix of $\boldsymbol{R}$, respectively. Substituting Eq. (11) and $I=\boldsymbol{V}\boldsymbol{V}^{-1}$ into Eq. (10), we have

$$(\boldsymbol{I}+\mathrm{i}\omega\boldsymbol{\Lambda}^{-1})\boldsymbol{y}'=\boldsymbol{H}',\tag{12}$$

where $\boldsymbol{y}'=\boldsymbol{V}^{-1}\boldsymbol{y}$ and $\boldsymbol{H}'=\boldsymbol{\Lambda}^{-1}\boldsymbol{V}^{-1}\boldsymbol{H}$.

From Eq. (12), we can write

$$(1+\mathrm{i}\omega\lambda_j^{-1})y_j'=h_j',\quad j=1,2,\ldots,N,\tag{13}$$

where $\lambda_j$ is the eigenvalue of $R$; $y_j'=\sum_{k=1}^{N}V_{jk}'y_k$ and $h_j'=\lambda_j^{-1}\sum_{k=1}^{N}V_{jk}'h_k$ are the entries of matrices $\boldsymbol{y}'$ and $\boldsymbol{H}'$, respectively, and $V_{jk}'$ is the entry of matrix $\boldsymbol{V}^{-1}$. We can rewrite Eq. (13) as

$$y_j'=\frac{h_j'}{(1+\mathrm{i}\omega\lambda_j^{-1})},\quad j=1,2,\ldots,N.\tag{14}$$

Since $\boldsymbol{y}'=\boldsymbol{V}^{-1}\boldsymbol{y}$, we have $\boldsymbol{y}=\boldsymbol{V}\boldsymbol{y}'$, that is

$$y_j=\sum_{n=1}^{N}V_{jn}y_n',\quad j=1,2,\ldots,N,\tag{15}$$

where $V_{jn}$ is the entry of matrix $\boldsymbol{V}$. Combing Eq. (14) and Eq. (15), we have

$$y_j = \sum_{n=1}^{N} \frac{V_{jn} h'_n}{(1+\mathrm{i}\omega\lambda_n^{-1})}, \quad j = 1,2,\ldots,N. \tag{16}$$

It is necessary to point out that in our previous work,[3] we obtained the numerical result of $y_j$ by solving Eq. (10) directly. In this paper, we give the analytical solution (Eq. (16)).

### 3.2. Decoupled expression of effective IMH for the sum of decoupled single-relaxation processes

By using Eq. (16), the effective IMH (Eq. (4)) can be expressed as

$$C_V^{\mathrm{eff}} = C_{\mathrm{mix}}^{\infty} + \sum_{n=1}^{N} \frac{h'_n \sum\limits_{j=1}^{N} a_j C_j^{\mathrm{vib}} V_{jn}}{(1+\mathrm{i}\omega\lambda_n^{-1})}. \tag{17}$$

Furthermore, we can rewrite Eq. (17) as

$$C_V^{\mathrm{eff}} = C_{\mathrm{mix}}^{\infty} + \sum_{n=1}^{N} \frac{C_n^*}{(1+\mathrm{i}\omega\tau_n)}, \quad C_n^* = h'_n \sum_{j=1}^{N} a_j C_j^{\mathrm{vib}} V_{jn},$$
$$\tau_n = \lambda_n^{-1}, \quad n = 1,2\cdots N. \tag{18}$$

Shield[7] and Bass[4,15] have pointed out that $C_V^{\mathrm{eff}}$ for a multimode vibrational relaxation can be expressed in a standard expression $C_V^{\mathrm{eff}} = C_{\mathrm{mix}}^{\infty} + \sum\limits_n C_n^*/(1+\mathrm{i}\omega\tau_n)$, where $C_n^*$ and $\tau_n$ are the vibrational IMH and the isothermal relaxation time for one of the decoupled single-relaxation processes, respectively. Compared with the standard expression given by them, equation (18) indicates that sound propagation would arouse $N$ single-relaxation processes in the mixture. Since each of the $N$ vibrational modes can provide a deexcitation path by its V–T energy transfer for the resident acoustic energy, the number $N$ in Eqs. (15)–(17) represents the quantity of the decoupled single-relaxation processes rather than the quantity of the vibrational modes.

Moreover, according to Eq. (18), each $C_n^*$ contains a part of the mole-fraction IMHs of all the vibrational modes in the mixture, which has resulted from the V–V energy coupling. On the other hand, each $\tau_n$ includes the lifetimes of all excited states which depend upon the transition probabilities of all V–T and V–V energy transitions, so it would not be possible to allocate a relaxation time to a particular vibrational mode.[7,15] Therefore, it is clear that the V–V energy coupling strongly influences both the relaxation time and the relaxation strength, which typically controls the multimode relaxation.[5]

We can define one of these $N$ decoupled single-relaxation processes as the decoupled process and the decoupled IMH $C_n^*$ as the process IMH for the $n$-th decoupled process, so $\tau_n$ is the corresponding relaxation time of this decoupled process. Consequently, based on Eq. (18), the multimode relaxation is the sum of its decoupled processes, and the number of decoupled processes is equal to the vibrational mode number.

In addition, according to Eq. (4), $y_j$ represents the contribution of $a_j C_j^{\mathrm{vib}}$ for $C_V^{\mathrm{eff}}$, thus $V_{jn}h'_n/(1+\mathrm{i}\omega\lambda_n^{-1})$ in Eq. (16) is the contribution of $a_j C_j^{\mathrm{vib}}$ in the $n$-th decoupled process for $C_V^{\mathrm{eff}}$. This implies that the contribution of a vibrational mode for the mixture's effective IMH is the sum of its contributions in all decoupled processes. As a result, equation (16) is the key intermediate step to decouple the coupled relaxation equations, and equation (18) is the accomplishment of decoupling the V–V coupling.

### 3.3. Sound absorption spectrum based on the decoupled models

The total sound absorption coefficient $\alpha$ of a gas medium is composed of the classical contribution $\alpha_{\mathrm{c}}$ connecting with the thermo-viscous effects and the relaxational contribution $\alpha_{\mathrm{r}}$, that is $\alpha = \alpha_{\mathrm{c}} + \alpha_{\mathrm{r}}$.[11,15] Therefore, $\alpha_{\mathrm{c}}$ can be omitted in studying the relaxational phenomena without loss of generality.[6]

In view of Eqs. (4) and (9), the temperature fluctuation ratio $y_j$ $(j = 1,2,\ldots,N)$ relates the micro molecular multimode relaxation with the macro effective IMH of the gas mixture. We can show the relationship between the effective IMH and the sound relaxational absorption by the effective thermodynamic sound speed $c_{\mathrm{e}}$[2,12]

$$c_{\mathrm{e}} = \sqrt{\frac{P_0}{\rho_0}\gamma^{\mathrm{eff}}} = \sqrt{\frac{P_0}{\rho_0}\frac{C_V^{\mathrm{eff}}+R}{C_V^{\mathrm{eff}}}}, \tag{19}$$

where $\gamma^{\mathrm{eff}}$ is the IMH ratio, and $P_0$ and $\rho_0$ are the equilibrium density and pressure, respectively. Since $C_V^{\mathrm{eff}}$ is complex, based on Eq. (19), $c_{\mathrm{e}}$ is complex as well. Furthermore, the sound propagation in an excitable gas can be characterized in terms of a complex-valued effective wave number $k_{\mathrm{e}}$, its real and imaginary parts yield the frequency-dependent phase speed $c$ and the relaxational absorption $\alpha_{\mathrm{r}}$, respectively.[2,6] By using the relationship between $k_{\mathrm{e}}$ and $c_{\mathrm{e}}$, we have

$$k_{\mathrm{e}} = \frac{\omega}{c} - \mathrm{i}\alpha_{\mathrm{r}} = \frac{\omega}{c_{\mathrm{e}}}. \tag{20}$$

Since the presence of relaxing gases is manifested by the relaxational peaks in the dimensionless absorption coefficient $\alpha\lambda$ ($\lambda$ is the sound wavelength) against the sound frequency $f$,[1] $\alpha\lambda$ can be used to emphasize the relaxational effects on the sound absorption.[3] We conventionally call $\alpha\lambda$ against $f$ the sound absorption spectrum. By using the last equality in Eq. (20), $\alpha_{\mathrm{r}}\lambda$ is given by

$$\alpha_{\mathrm{r}}\lambda = -2\pi\mathrm{Im}(c_{\mathrm{e}}^{-1})/\mathrm{Re}(c_{\mathrm{e}}^{-1}). \tag{21}$$

Based on Eq. (18), for simplicity, we write

$$C_V^{\mathrm{eff}} = x(\omega) - \mathrm{i}y(\omega), \tag{22}$$

where

$$x(\omega) = C_{\text{mix}}^{\infty} + \sum_{n=1}^{N} \frac{C_n^*}{1+(\omega\tau_n)^2},$$

and

$$y(\omega) = \sum_{n=1}^{N} \frac{\omega\tau_n C_n^*}{1+(\omega\tau_n)^2}.$$

Substituting Eq. (22) into Eq. (19) and based on Eq. (21), we can get the analytical expression for $\alpha_r\lambda$ as[3]

$$\alpha_r\lambda = 2\pi\{[(B/C)^2+1]^{1/2} - B/C\}, \tag{23}$$

where $B = x^2(\omega) + y^2(\omega) + Rx(\omega)$, and $C = Ry(\omega)$.

## 4. Simulations and discussion

To validate our proposed model, we need to compare the results with experiment data. The necessary parameters for the prediction of our decoupling model are given in Table 1, which provides the normal vibrational modes and the degeneracies ($g$) of nitrogen, oxygen, chlorine, methane, and carbon dioxide. The calculation results of mode IMHs in Table 1 will be compared with the results of decoupled process IMHs in Subsections 4.1 and 4.2.

**Table 1.** Normal vibrational modes and mode degeneracies $g$ for selected gases (Refs. [1] and [16]), and the corresponding vibrational isochoric molar heats (IMHs) calculated by the Planck–Einstein function (Eq. (2)) around room temperature.

| Gas | Normal mode of vibration $\upsilon$/cm$^{-1}$ | $g$ | Vibrational IMH | |
|---|---|---|---|---|
| | | | $T$/K | $C_V^{\text{vib}}$/J·mol$^{-1}$·K$^{-1}$ |
| $N_2$ | $\upsilon = 2331$ | 1 | 297 | $1.32\times10^{-2}$ |
| $O_2$ | $\upsilon = 1554$ | 1 | 303.2 | $2.83\times10^{-1}$ |
| $Cl_2$ | $\upsilon = 577$ | 1 | 296.2 | 4.48 |
| $CH_4$ | $\upsilon_4 = 1306$ | 3 | 299.15 | 1.84 |
| | $\upsilon_2 = 1534$ | 2 | | $5.65\times10^{-1}$ |
| | $\upsilon_1 = 2915$ | 1 | | $1.30\times10^{-3}$ |
| | $\upsilon_3 = 3019$ | 3 | | $8.61\times10^{-5}$ |
| $CO_2$ | $\upsilon_2 = 677$ | 2 | 296.15 | 7.39 |
| | $\upsilon_1 = 1388$ | 1 | | $4.45\times10^{-1}$ |
| | $\upsilon_3 = 2349$ | 1 | | $1.19\times10^{-2}$ |

In Table 1, the number of normal vibrational modes (usually called vibrational modes) is equal to the required DOF to describe the vibrational motion, so the number is $3H$–5 for a linear molecule (e.g., $N_2$, $CO_2$) and $3H$–6 for a nonlinear molecule (e.g., $CH_4$), where $H$ is the number of atoms. Each vibrational mode, treated as a simple oscillator, has a defined vibrational frequency. If the same frequency is shared by 2 or 3 vibrational modes of a molecule, these modes are considered to be degenerate. The vibrational frequencies of the normal modes are expressed in the spectroscopic convention with the inverse wavelength, which gives the value in units of frequency (Hz) after multiplying with the speed of light ($3\times10^{10}$ cm/s).

### 4.1. Simulations of sound absorption spectrum under one-mode vibrational relaxation

To verify our model, we first consider the sound absorption in a pure diatomic gas, which has only one vibrational mode to arouse a single-relaxation process. Since the relaxation time varies inversely with the ambient pressure, raising the sound frequency is equivalent to lowering the pressure.[2,17] The sound absorption spectrum can be traditionally plotted as a function of the frequency–pressure ratio $f/P$. Figure 1 presents the comparison of predicted absorption spectra with the experimental data for three kinds of pure diatomic gases, nitrogen, oxygen, and chlorine; the corresponding calculation results of the process IMHs and the relaxation times are provided in Table 2.

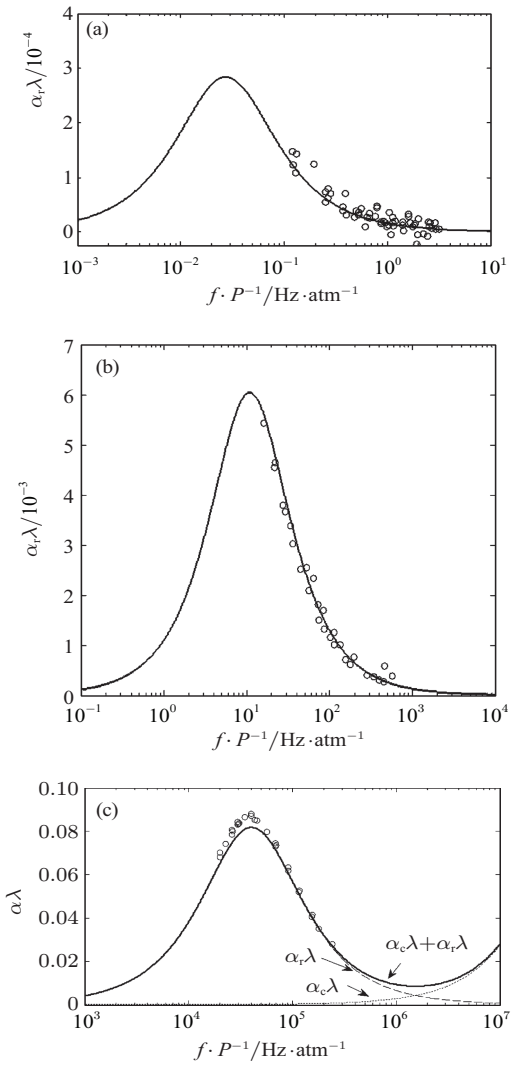



**Fig. 1.** (a) Relaxational absorption for $N_2$, experimental data from Zuckerwar[19] ($T = 297$ K), (b) relaxational absorption for $O_2$, experimental data from Holmes[20] ($T = 303.2$ K), (c) total absorption (solid), relaxational absorption (dashed), classical absorption (dotted) for $Cl_2$, and experimental data from Shields[21] ($T = 296.2$ K). Curves represent the spectra predicted by the model around room temperature, and symbols represent the experimental data.

Figures 1(a) and 1(b) show the comparison results for $N_2$ and $O_2$, respectively. Since the relaxation frequencies of $N_2$ ($\sim$0.01 Hz) and $O_2$($\sim$10 Hz) are below the measurement capability, the experimental data cannot match the actual absorption peaks in Figs. 1(a) and 1(b). Nevertheless, our predictions are very consistent with the uncompleted data, and cover the frequency ranges undetected by the experiments. The low relaxation frequencies ($< 10$ Hz) of these two gases make the classical absorption negligible over the frequency range where their relaxational parts are dominant. The predicted spectrum is also quite consistent with the experimental data for $Cl_2$ in Fig. 1(c), where the total sound absorption $\alpha\lambda$ (bold solid) is divided into two parts: the relaxational absorption $\alpha_r\lambda$ (fine dashed) and the classical absorption $\alpha_c\lambda$ (fine dotted). The latter is calculated with the Stokes and Kirchhoff formulation,[18] and is quite small compared with the former at $f/P < 10^6$ Hz$\cdot$atm$^{-1}$. However, at higher values of $f/p$, $\alpha_c\lambda$ rapidly becomes dominant. Therefore, the classical absorption generally plays a role at frequencies in the megahertz range, while the relaxational absorption is dominant at moderate frequencies.[1]

The comparison between the data in Tables 2 and 1 shows that the process IMHs and the corresponding vibrational IMHs are identical for a given diatomic gas at the same temperature. Since the V–V exchange is invalid for the case of one mode, the mode can only relax the stored energy through its V–T transfer to arouse one single-relaxation process. This means that the vibrational mode and the relaxation process have a one-to-one correlation in a diatomic gas.

**Table 2.** Calculation results of process IMHs and relaxation times for three pure diatomic gases around room temperature.

| Gas | $T$/K | $C_1^*$/J$\cdot$mol$^{-1}\cdot$K$^{-1}$ | $\tau_1$/s |
|---|---|---|---|
| $N_2$ | 297 | $1.32\times10^{-2}$ | 5.80 |
| $O_2$ | 303.2 | $2.83\times10^{-1}$ | $1.49\times10^{-2}$ |
| $Cl_2$ | 296.2 | 4.48 | $4.69\times10^{-6}$ |

### 4.2. Simulations of sound absorption spectrum under multimode vibrational relaxation

Furthermore, we can test the predicted sound absorption spectra under multimode vibrational relaxations. The sound absorption spectra of $CO_2$–$O_2$, $CO_2$–$N_2$, $CH_4$–$N_2$, $CO_2$, and $CH_4$ are depicted in Fig. 2. Table 1 provides the corresponding calculation results of the process IMHs and the relaxation times for those gases.

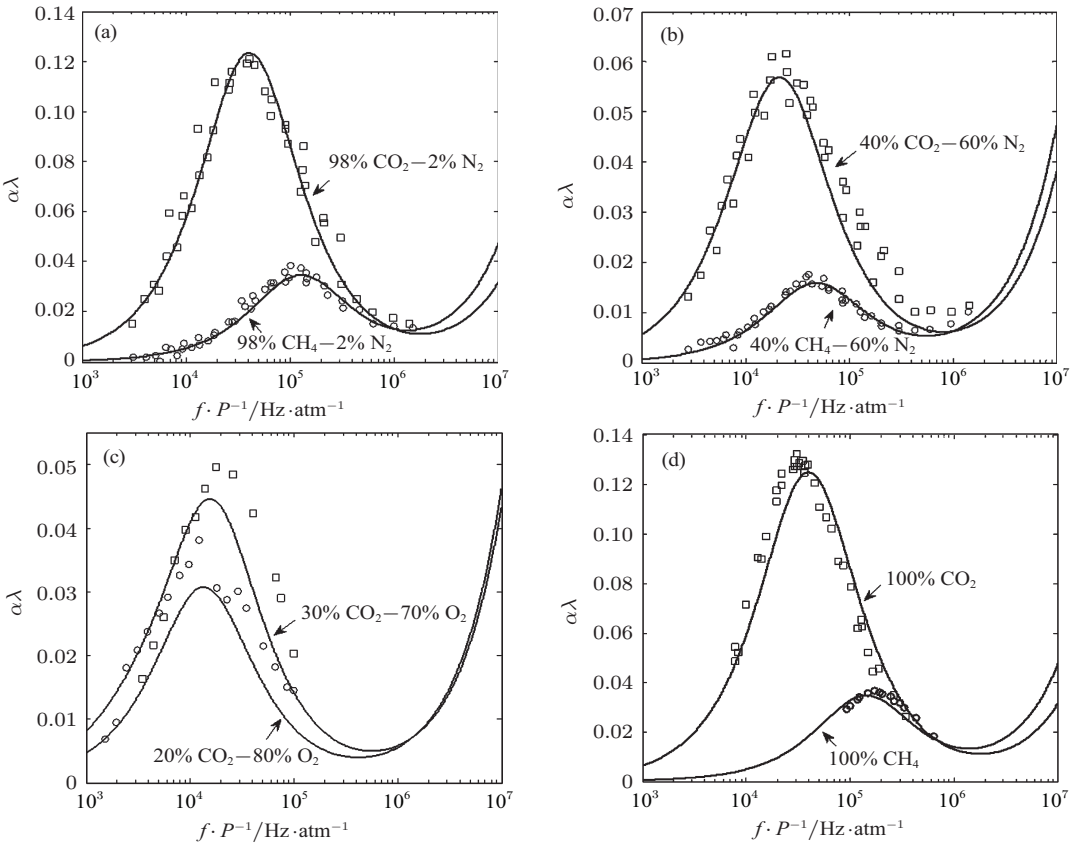



**Fig. 2.** Comparison of predicted sound absorption spectra (curves) with experimental data (symbols) for several excitable gases with the multiple modes around room temperature. (a) Sound absorptions for 98% $CO_2$–2% $N_2$ and 98% $CH_4$–2% $N_2$, experimental data from Petculescu[22] (circle: 98% $CH_4$–2% air, $T = 300$ K; square: 98% $CO_2$–2% air, $T = 298$ K); (b) sound absorptions for 40% $CO_2$–60% $N_2$ and 40% $CH_4$–60% $N_2$, experimental data from Ejakov[16] (circle: 40% $CH_4$–60% $N_2$, $T = 293$ K; square: 40% $CO_2$–60% $N_2$, $T = 293.7$ K); (c) sound absorption for $CO_2$–$O_2$, experimental data from Bass[23] (circle: 20% $CO_2$–80% $O_2$, $T = 300$ K; square: 30% $CO_2$–70% $O_2$, $T = 300$ K); (d) sound absorptions for 100% $CO_2$ and 100% $CH_4$, experimental data from Gravitt[24] (circle: 100% $CH_4$, $T = 299.15$ K) and Angona[25] (square: 100% $CO_2$, $T = 296.15$ K).

The comparison results of 98% $CO_2$–2% $N_2$ and 98% $CH_4$–2% $N_2$ in Fig. 2(a) and 40% $CO_2$–60% $N_2$ and 40% $CH_4$–60% $N_2$ in Fig. 2(b) show that the predicted spectra are consistent with the experimental data. For 30% $CO_2$–70% $O_2$ and 20% $CO_2$–80% $O_2$ in Fig. 2(c), the amplitudes of the calculated spectra are slightly smaller than the experimental data. For pure $CO_2$ and pure $CH_4$ in Fig. 2(d), only the positions of the predicted absorption peaks differ a little from the experimental data. These discrepancies may result from the sensitivity of absorption in gases to impurities. In particular, a small amount of water can cause a large shift in the relaxation peak.[16] In summary, by combining the results in Figs. 1 and 2, it is clear that our predicted absorption spectra agree very well with the experimental data, which validates our proposed model.

### 4.3. Discussion of the relationship between sound absorption spectra and the decoupled processes

#### 4.3.1. Characteristics of the decoupled processes

Firstly, we analyze the calculation results in Table 3 to reveal several characteristics of the decoupled processes of a multimode relaxation in a polyatomic gas/gas mixture.

(i) According to Eqs. (4) and (18), the quantity of the decoupled processes with different process IMHs and relaxation times is the same as the number of vibrational modes for a given gas/mixture. For example, the 98% $CO_2$–2% $N_2$ mixture has four vibrational modes as shown in Table 1, those modes can form the four decoupled processes with different relaxation times in Table 3. Hence, strictly speaking, a single relaxation or single-relaxation-time process can only happen in a pure diatomic gas; while any multimode relaxation in a polyatomic gas or mixture must be a multi-relaxation process.

(ii) It would be impossible to find a process IMH $C_n^*$ that is entirely equal to the mole-fraction IMH $a_j C_j^{\mathrm{vib}}$ of any particular vibrational mode (based on Eq. (2)). For example, the process IMHs in Table 3 of pure $CH_4$ or pure $CO_2$ and the corresponding vibrational IMHs in Table 1 are all different. As shown by Eq. (18), after the coupling of the V–V energy exchanges, a process IMH contains parts of the mole-fraction IMHs of all vibrational modes.

Since the vibrational relaxation is essentially a series of energy redistributions,[26] according to characteristics (i) and (ii) , a multimode relaxation is determined by two kinds of energy transitions: the V–V exchanges and the V–T transfer. On one hand, since only the V–T transfer can provide the deexcitation paths for the resident acoustic energy to the translational motion, it is possible to allocate the deexcitation path of a decoupled process to a certain vibrational mode. Therefore, the quantity of the decoupled processes is the same as the number of the vibrational normal modes. On the other hand, the rapid V–V exchanges strongly couple the stored energy of all vibrational modes, as a result of which every process IMH contains the contributions of all vibrational modes. Therefore, it is impossible to assign the process IMH or the relaxation time of a decoupled process to a particular vibrational mode. Consequently, from the view of the deexcitation path for the relaxing energy of a decoupled process, a decoupled process corresponds to a particular mode; while from the view of the composition for the relaxing energy of a decoupled process, a decoupled process is related to all vibrational modes.

(iii) The process IMH value of the 1st decoupled process is much larger than that of the other processes in Table 3, and almost equal to the whole contribution of the relaxation energy of all vibrational modes, i.e. $C_1^* \approx \sum_{j=1}^{N} a_j C_j^{\mathrm{vib}}$. Thus, the first decoupled process is the primary process.

**Table 3.** Calculation results of process IMHs and relaxation times of the decoupled processes in the gas media shown in Fig. 2 (at the same temperature for a given gas/mixture).

| Gas | 1st process | | 2nd process | | 3rd process | | 4th process | | 5th process | |
|---|---|---|---|---|---|---|---|---|---|---|
| | $C_1^*/$ J·mol$^{-1}$·K$^{-1}$ | $\tau_1$/s | $C_2^*/$ J·mol$^{-1}$·K$^{-1}$ | $\tau_2$/s | $C_3^*/$ J·mol$^{-1}$·K$^{-1}$ | $\tau_3$/s | $C_4^*/$ J·mol$^{-1}$·K$^{-1}$ | $\tau_4$/s | $C_5^*/$ J·mol$^{-1}$·K$^{-1}$ | $\tau_5$/s |
| 20% $CO_2$ –80% $O_2$ | 1.48 | $1.23\times10^{-5}$ | 0.159 | $2.41\times10^{-4}$ | $7.52\times10^{-4}$ | $2.29\times10^{-2}$ | $-1.44\times10^{-4}$ | $1.89\times10^{-6}$ | – | – |
| 30% $CO_2$ –70% $O_2$ | 2.17 | $1.08\times10^{-5}$ | 0.232 | $5.94\times10^{-5}$ | $1.11\times10^{-3}$ | $2.02\times10^{-2}$ | $-3.16\times10^{-4}$ | $1.80\times10^{-6}$ | – | – |
| 40% $CH_4$ –60% $N_2$ | 0.85 | $3.43\times10^{-6}$ | $4.76\times10^{-3}$ | $1.41\times10^{-6}$ | $-3.36\times10^{-6}$ | $6.06\times10^{-10}$ | $-7.44\times10^{-8}$ | $8.96\times10^{-9}$ | $1.16\times10^{-10}$ | $2.31\times10^{-9}$ |
| 40% $CO_2$ –60% $N_2$ | 2.30 | $7.64\times10^{-6}$ | $7.06\times10^{-1}$ | $1.18\times10^{-5}$ | $3.25\times10^{-3}$ | 1.60 | $-1.14\times10^{-9}$ | $2.80\times10^{-6}$ | – | – |
| 98% $CH_4$ –2% $N_2$ | 2.32 | $1.37\times10^{-6}$ | $-4.23\times10^{-5}$ | $2.89\times10^{-7}$ | $-4.51\times10^{-6}$ | $1.15\times10^{-10}$ | $-1.26\times10^{-7}$ | $1.88\times10^{-9}$ | $9.01\times10^{-11}$ | $4.08\times10^{-10}$ |
| 98% $CO_2$ –2% $N_2$ | 7.45 | $5.15\times10^{-6}$ | $3.23\times10^{-2}$ | $1.51\times10^{-6}$ | $3.34\times10^{-3}$ | $9.26\times10^{-2}$ | $-3.54\times10^{-8}$ | $1.75\times10^{-6}$ | – | – |
| 100% $CH_4$ | 2.34 | $1.36\times10^{-6}$ | $-4.43\times10^{-6}$ | $1.11\times10^{-10}$ | $-1.22\times10^{-7}$ | $1.82\times10^{-9}$ | $8.19\times10^{-11}$ | $3.93\times10^{-10}$ | – | – |
| 100% $CO_2$ | 7.57 | $5.01\times10^{-6}$ | $3.13\times10^{-2}$ | $1.45\times10^{-6}$ | $3.25\times10^{-3}$ | $9.08\times10^{-2}$ | – | – | – | – |

This kind of behavior is shown by most of the excitable gases. The picture is that the energy gaps between the upper modes are usually much smaller than the energy level of the lowest mode (which has the lowest vibrational frequency), and thus the rapid V–V exchanges maintain the continuous equilibrium of vibrational energy among all vibrational modes.[1] As a result, almost all vibrational energy relaxes through the V–T transfer of the lowest mode because of its fastest V–T transition rate $k_{10}(j)$. And this is why the process IMH of the primary process is almost equal to the overall contribution of the relaxing vibrational modes. For example, there are five decoupled processes in the 98% $CH_4$–2% $N_2$ mixture. The IMH of the 1st process (2.34 $J \cdot mol^{-1} \cdot K^{-1}$ is much larger than the others, and it is obvious that the value is almost equal to the sum of the mole-fraction IMHs of all modes. This means that almost the whole vibrational energy relaxes through the V–T deexcitation path of the mode $CH_4$ ($\upsilon_4 = 1306$). Therefore, the resident energy relaxed by the primary process generally selects the V–T deexcitation path provided by the lowest mode.

In addition, the process IMHs of some non-primary processes have quite small negative values in Table 3. This indicates that it is possible for a higher vibrational mode, which provides the V–T deexcitation path for a non-primary decoupled process, to acquire slightly more energy in its V–V exchanges than the relaxing amount acquired by its V–T transfer.

#### 4.3.2. Interpretation of the sound absorption spectrum with only one peak

Secondly, we use the above characteristics of the decoupled processes to explain the features presented by the sound absorption spectra in Fig. 2.

1) There is only one absorption peak corresponding to one decoupled process for a given gas/mixture. Since the process IMH of a decoupled process reflects the amount of acoustic energy relaxing through this process until the thermal equilibrium has been attained, the higher process IMH means that the larger amount of acoustic energy would be relaxed as heat. That is, the higher process IMH produces the higher sound absorption peak. Based on characteristic (i), there are four decoupled processes and there should be four absorption spectral peaks for 40% $CO_2$–60% $N_2$. However, actually only one peak can be found in Fig. 2(b). According to characteristic (ii), the very small process IMHs of the non-primary decoupled processes mean they may not be observed in the absorption spectra. Meanwhile, only $C_1^*$ of the primary process is significant, which is almost equal to the sum of the IMHs of all vibrational modes. Consequently, the only peak of every spectrum in Fig. 2 is exactly the result from the primary process.

2) For the mixture of $CH_4$–$N_2$ or $CO_2$–$N_2$ in Fig. 2, the absorption peak increases in amplitude as the fraction of $CH_4$ or $CO_2$ increases. We find that the process IMH of the 1st process is also gradually increased in Table 3. For example, the process IMH of the 1st process is 7.45 $J \cdot mol^{-1} \cdot K^{-1}$ for 98% $CH_4$–2% $N_2$, and it becomes 2.30 $J \cdot mol^{-1} \cdot K^{-1}$ for 40% $CH_4$–60% $N_2$, while the absorption peak of the former (about 0.12) is two times higher than that of the latter (about 0.06). Likewise, the 1st process IMH of a mixture consisting of $CO_2$ is more than that of a mixture having $CH_4$ with the same mole fraction according to Table 3, and this leads to a higher spectral peak of the former rather than the latter in Figs. 2(a), 2(b), and 2(d). Since the larger process IMH means the more resident energy relaxing as heat, the amplitude of an absorption peak is proportional to the primary process IMH.

3) The sound frequency of an absorption peak (the relaxation frequency) increases as the relaxation time of the 1st process decreases. For example, according to Table 3, the relaxation time of the 1st process in pure $CH_4$ is less than that in pure $CO_2$, and thus the relaxation frequency of the former is obviously higher than that of the latter in Fig. 2(d). Similarly, the relaxation time of the 1st process in the mixture of $CH_4$–$N_2$ decreases as the fraction of $CH_4$ increases, the position of the absorption peak gradually moves to the right. Thereby, the frequency of the absorption peak is inversely proportional to the relaxation time of the primary process.

Furthermore, we can find the analytical relationship between the relaxation frequency and the relaxation time for a decoupled process. When just considering the $n$-th decoupled process, based on Eq. (23), we put $\mathrm{d}(B/C)/\mathrm{d}\omega = 0$, then obtain the minimum point of $B/C$ when $\omega = 2\pi f_n^{\mathrm{relax}}$, which corresponds to the maximum point of the sound absorption. Thus, the relaxation frequency for the $n$-th decoupled process is[3]

$$f_n^{\mathrm{relax}} = \frac{1}{2\pi\tau_n}\sqrt{\frac{(C_{\mathrm{mix}}^{\infty}+C_n^*)(C_{\mathrm{mix}}^{\infty}+C_n^*+R)}{C_{\mathrm{mix}}^{\infty}(C_{\mathrm{mix}}^{\infty}+R)}}. \tag{24}$$

The same view of Eq. (24) is also given by Bauer,[2] Herzfeld,[11] and Shield[7] for a single-relaxation process. Thus when the relationship between the relaxation time and the sound frequency satisfies Eq. (24), the absorption peak emerges. Therefore, this reconfirms that the freqency of the peak or the relaxation frequency varies inversely with the relaxation time.

However, the DL group inadvertently believed that the relationship between $f_n^{\mathrm{relax}}$ and $\tau_n$ was $f_n^{\mathrm{relax}} = (2\pi\tau_n)^{-1}$.[6,8] In fact, the sound propagation in a gaseous medium is an adiabatic process, but $\tau_n$ is the relaxation time of the isothermal process directly related to the molecular energy transfer.[1] Hence there is a confusion about those two processes for the relationship $f_n^{\mathrm{relax}} = (2\pi\tau_n)^{-1}$. As an example, according to Petculescu experimental data in Fig. 2(a), the relaxation frequency of the primary process in 98% $CH_4$–2% $N_2$ is $4.05 \times 10^4$ Hz, and on the basis of Eq. (24), the theoretical result is $4.07 \times 10^4$ Hz, but using the relationship of the DL model, the result becomes $3.09 \times 10^4$ Hz, which has about a 25% relative error.

#### 4.3.3. Interpretation of the sound absorption spectrum with more than one peak

Thirdly, to further elucidate how the decoupled processes affect a sound absorption spectrum, we show the spectra with more than one peak for the ternary mixtures of 2% $CO_2$–2% $Cl_2$–96% $N_2$ and 2% $CO_2$–3% $Cl_2$–95% $N_2$ ($T = 297$ K) in Fig. 3. The corresponding calculation results of the process IMHs, relaxation times, and relaxation frequencies are listed in Tables 4 and 5, respectively. For 2% $CO_2$–2% $Cl_2$–96% $N_2$, according to Table 4, there are only two significant decoupled processes ($C_1^* = 0.149\,\mathrm{J\cdot mol^{-1}\cdot K^{-1}}$ and $C_2^* = 0.087\,\mathrm{J\cdot mol^{-1}\cdot K^{-1}}$; $\tau_1 = 9.66\times10^{-6}$ s and $\tau_2 = 9.30\times10^{-6}$ s) among the five total decoupled processes. They correspond to the two peaks ($f_1^{\mathrm{relax}} = 16.6$ kHz and $f_2^{\mathrm{relax}} = 172$ kHz) in Fig. 3. As the fraction of $Cl_2$ increases to 3% and that of $N_2$ decreases to 95%, the amplitudes of the two peaks rise, and the frequency of the 1st peak shifts to a higher value ($f_1^{\mathrm{relax}'} = 18.6$ kHz) while the 2nd peak moves to a lower value ($f_2^{\mathrm{relax}'} = 169$ kHz). In Table 5, we find that there are still only two significant decoupled processes, i.e. the 1st and the 2nd processes are important, the corresponding process IMHs become larger ($C_1^* = 0.150\,\mathrm{J\cdot mol^{-1}\cdot K^{-1}}$ and $C_2^* = 0.129\,\mathrm{J\cdot mol^{-1}\cdot K^{-1}}$, and the relaxation time of the 1st process decreases while that of the 2nd process increases ($\tau_1' = 8.62\times10^{-6}$ s and $\tau_2' = 9.49\times10^{-6}$ s). Therefore, the amplitude of an absorption peak is proportional to the corresponding process IMH, while the frequency of the absorption peak varies inversely with the relaxation time. It is this property of the sound absorption spectrum varying with the gas composition that allows a possible way to continuously sense gas composition by the acoustic measurements.[27–30]

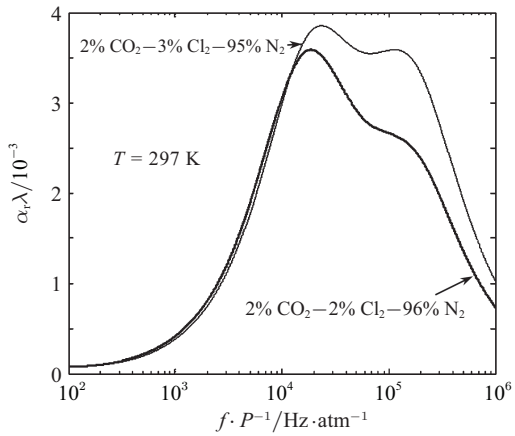



**Fig. 3.** Sound relaxational absorption spectra for 2% $CO_2$–2% $Cl_2$–96% $N_2$ and 2% $CO_2$–3% $Cl_2$–95% $N_2$.

Above all, a multimode relaxation process is the sum of its decoupled single-relaxation processes with different relaxation times, and it is a multi-relaxation process in nature. Furthermore, whether one of those decoupled processes displaying as a peak in the sound absorption spectrum is decided by the value of its process IMH; and the amplitude and the frequency of an absorption peak are determined by the process IMH and the relaxation time of the corresponding decoupled process, respectively.

**Table 4.** Calculation results of the process IMHs, relaxation times, and relaxation frequencies of the five decoupled processes for the 2% $CO_2$–2% $Cl_2$–96% $N_2$ mixture ($T = 297$ K).

| Process | 1st | 2nd | 3rd | 4th | 5th |
|---|---|---|---|---|---|
| $C_n^*$ /J·mol$^{-1}$·K$^{-1}$ | $1.49\times10^{-1}$ | $8.71\times10^{-2}$ | $1.26\times10^{-2}$ | $8.41\times10^{-3}$ | $-4.76\times10^{-11}$ |
| $\tau_n$/s | $9.66\times10^{-6}$ | $9.30\times10^{-7}$ | 6.07 | $6.64\times10^{-1}$ | $1.26\times10^{-6}$ |
| $f_n^{\mathrm{relax}}$/Hz | $1.66\times10^{4}$ | $1.72\times10^{5}$ | $2.62\times10^{-2}$ | 24.0 | $1.27\times10^{5}$ |

**Table 5.** Calculation results of the process IMHs, relaxation times, and relaxation frequencies of the five decoupled processes in the 2% $CO_2$–3% $Cl_2$–95% $N_2$ mixture ($T = 297$ K).

| Process | 1st | 2nd | 3rd | 4th | 5th |
|---|---|---|---|---|---|
| $C_n^*$/J·mol$^{-1}$·K$^{-1}$ | $1.50\times10^{-1}$ | $1.29\times10^{-1}$ | $1.24\times10^{-2}$ | $4.07\times10^{-3}$ | $-4.76\times10^{-11}$ |
| $\tau_n$/s | $8.62\times10^{-6}$ | $9.49\times10^{-7}$ | 6.19 | $6.47\times10^{-1}$ | $1.28\times10^{-6}$ |
| $f_n^{\mathrm{relax}}$/Hz | $1.86\times10^{4}$ | $1.69\times10^{5}$ | $2.57\times10^{-1}$ | 24.6 | $1.27\times10^{5}$ |

## 5. Conclusions

In this paper, we have presented a model to decouple the coupled energy relaxation equations to calculate the process IMHs and the relaxation times of the decoupled single-relaxation processes of a multimode relaxation in multicomponent gas mixtures. At room temperature, the sound absorption spectra based on the proposed decoupling model are consistent with the experimental data for the mixtures of $CO_2$–$O_2$, $CO_2$–$N_2$, and $CH_4$–$N_2$, and pure gases of $N_2$, $O_2$, $Cl_2$, $CO_2$, and $CH_4$ quite well. Those comparisons verify the validity of the model. Meanwhile, we use the characteristics of those decoupled processes to quantitatively articulate the interplay between the sound absorption spectrum and molecular

multimode relaxation.

We have demonstrated that a multimode relaxation is the sum of its decoupled single-relaxation processes with different relaxation times. From the view of the V–T deexcitation path for a decoupled process, the number of the decoupled processes is the same as that of the vibrational modes. While from the view of the V–V coupled energy for a decoupled process, a process IMH contains parts of the mole-fraction IMHs of all vibrational modes, and hence a decoupled process is related to all vibrational modes.

In a multi-component gas mixture, the nature behind the relationship between a multimode vibrational relaxation and its sound absorption spectrum is the characteristics of its decoupled processes. We have quantitatively shown how the characteristics of the decoupled processes determine the features of the corresponding sound absorption spectra. First, the number of significant process IMHs determines the number of obvious peaks in the sound absorption spectrum. Second, the amplitude of an absorption peak is proportional to the process IMH, while the the peak frequency is inversely proportional to the relaxation time.

We find that the decoupling model provides a deep insight into the relationship between the sound absorption spectrum and the molecular vibrational relaxation in multi-component excitable gas mixtures. This model can be further used to separate a decoupled single-relaxation spectrum from a multi-relaxation spectrum to simplify the analysis of the relationship between the gas composition and sound absorption in gas mixtures.

## References


[1] Lambert J D 1977 *Vibrational and Rotational Relaxation in Gases* (Oxford: Clarendon) pp. 1–114
[2] Mason W P 1965 *Physical Acoustics* (Vol. II) (New York: Academic Press)
[3] Zhang K S, Wang S, Zhu M, Hu Y and Jia Y Q 2012 *Acta Phys. Sin.* **61** 174301 (in Chinese)
[4] Bauer H J, Shields F D and Bass H E 1972 *J. Chem. Phys.* **57** 4624
[5] Zuckerwar A J and Miller K W 1988 *J. Acoust. Soc. Am.* **84** 970
[6] Petculescu A G and Lueptow R M 2005 *Phys. Rev. Lett.* **94** 238301
[7] Shields F D 1970 *J. Acoust. Soc. Am.* **47** 1262
[8] Dain Y and Lueptow R M 2001 *J. Acoust. Soc. Am.* **109** 1955
[9] Petculescu A G and Lueptow R M 2005 *J. Acoust. Soc. Am.* **117** 175
[10] Schwartz R N, Slawsky Z I and Herzfeld K F 1952 *J. Chem. Phys.* **20** 1591
[11] Herzfeld K F and Litovitz T A 1959 *Absorption and Dispersion of Ultrasonic Waves* (New York: Academic) pp. 55–216
[12] Morse P M and Ingard K U 1968 *Theoretical Acoustics* (New York: McGraw-Hill) pp. 294–300
[13] Tanczos F I 1956 *J. Chem. Phys.* **25** 439
[14] Jia Y Q, Wang S, Zhu M, Zhang K S and Yuan F G 2012 *Acta Phys. Sin.* **61** 095101 (in Chinese)
[15] Bass H E, Bauer H J and Evans L B 1972 *J. Acoust. Soc. Am.* **52** 821
[16] Ejakov S G, Phillips S, Dain Y, Lueptow R M and Visser J H 2003 *J. Acoust. Soc. Am.* **113** 1871
[17] Phillips S, Dain Y and Lueptow R M 2003 *Meas. Sci. Technol.* **14** 70
[18] Lawrence E K, Austin R F, Alan B C and James V S 1982 *Fundamentals of Acoustics* (New York: Wiley) pp. 141–149
[19] Zuckerwar A J and Griffin W A 1980 *J. Acoust. Soc. Am.* **68** 218
[20] Holmes R, Smith F A and Tempest W 1963 *Proc. Phys. Soc.* **81** 311
[21] Shields F D 1959 *J. Acoust. Soc. Am.* **31** 248
[22] Petculescu A G, Hall B, Fraenzle R, Phillips S and Lueptow R M 2006 *J. Acoust. Soc. Am.* **120** 1779
[23] Bass H E 1973 *J. Chem. Phys.* **58** 4783
[24] Gravitt J C, Whetstone C N and Lagemann R T 1966 *J. Chem. Phys.* **44** 70
[25] Angona F A 1953 *J. Acoust. Soc. Am.* **25** 1116
[26] Yu G Y, Song Y F, He X, Zheng X X, Tan D W, Chen J and Yang Y Q 2012 *Chin. Phys.* B **21** 043402
[27] Petculescu A G and Lueptow R M 2012 *Sensors & Actuators*B: *Chemical* **169** 121
[28] Yan S, Wang S and Dou Z 2007 *Meas. Sci. Technol.* **18** 1278
[29] Yan S and Wang S 2008 *Acta Phys. Sin.* **57** 4282 (in Chinese)
[30] Zhu M, Wang S, Wang S T and Xia D H 2008 *Acta Phys. Sin.* **57** 5749 (in Chinese)